REDVET - Revista electrónica de Veterinaria - ISSN 1695-7504
Vol 25, No. 2 (2024)
http://www.veterinaria.org
Article Received Revised- Accepted-

Enhancement Of Mechanical And Tribological Behaviours Of AZ91D Magnesium Hybrid Composites Reinforced With B_4C/MWCNT Prepared By Stir Casting

Hemant Kumar Choudhary [1*], Akshay Sharma[2], Md Irshad Alam[3], Manhar Kumar Sah[4], Abhishek Kumar [5] and Pankaj Kumar[6]

[1*,3,4,6] Assistant Professor, Department of Mechanical Engineering, Muzaffarpur Institute of Technology, Muzaffarpur-842003, India. Email : hemant.in2@gmail.com, pankajraj2310@gmail.com, irshad.me@mitmuzaffarpur.org, mhrkmrsh@gmail.com

[2]Assistant Professor, Department of Mechanical Engineering, Government Engineering College, Bhojpur. gecakshay09.dstte@bihar.gov.in

[5]Assistant Professor, Department of Mechanical Engineering, Rashtrakavi Ramdhari Singh Dinkar College of Engineering, Begusarai. abhishekme10107@gmail.com

[*]**Corresponding Author**: Hemant Kumar Choudhary
*Assistant Professor, Department of Mechanical Engineering, Muzaffarpur Institute of Technology, Muzaffarpur-842003, India. Email: hemant.in2@gmail.com

Abstract
The inherent limitations of the AZ91D magnesium alloy, specifically its low hardness and poor wear resistance, necessitate the development of hybrid metal matrix composites (HMMCs) for high-performance structural applications. In this study, hybrid composites reinforced with a constant 1.5 wt. % B_4C microparticles and varying concentrations of multi-walled carbon nanotubes (MWCNTs) (0.2 and 0.4 wt. %) were successfully fabricated using the bottom-pouring stir casting technique under a protective Argon atmosphere. Microstructural characterization revealed that the hybrid reinforcements acted as effective nucleating agents, leading to significant grain refinement and a uniform distribution within the magnesium matrix. Density measurements showed a progressive reduction in porosity, reaching a minimum of 1.05% for the 0.4 wt. % MWCNT sample, indicating excellent interfacial bonding. Mechanical testing demonstrated a synergistic strengthening effect, with the microhardness increasing from 82.7 HV to 115.9 HV (a 40.1% improvement). Tribological evaluations conducted via pin-on-disc testing indicated a substantial decrease in the Coefficient of Friction (COF), dropping from 0.312 for the unreinforced alloy to 0.261 for the 0.4 wt. % MWCNT composite. The results suggest that while B_4C microparticles provide structural stiffness and load-bearing capacity, the MWCNTs contribute to nanoscale strengthening and the formation of a self-lubricating tribo-layer. This hybrid reinforcement strategy successfully balances mechanical strength and frictional efficiency, positioning these composites as ideal candidates for lightweight, wear-resistant components in the automotive and aerospace industries.

Keywords: Tribological behaviour, AZ91D magnesium alloy, Hybrid reinforcement, MWCNTs, B4C, Stir Casting, Coefficient of Friction (COF).

1. Introduction

The global demand for lightweight and high-performance structural materials is rapidly increasing across the aerospace, automotive, and biomedical industries, driven by the need for enhanced fuel efficiency and sustainability. Magnesium alloys stand out as prime candidates due to their exceptionally low density (approximately 33% lighter than aluminium and 75% lighter than steel) and high specific strength-to-weight ratio. Despite these compelling advantages, a major impediment to their widespread application, particularly in sliding or rotating mechanical components, is their inherent softness, low elastic modulus, and poor resistance to abrasive and adhesive wear, often leading to premature failure under dynamic operating conditions. To address this critical limitation, the development of Magnesium Matrix Composites (MMCs) has emerged as a successful and intensive research strategy. MMCs are fabricated by incorporating hard ceramic reinforcements, such as SiC, Al_2O_3, and TiC, to simultaneously enhance the hardness, stiffness, and tribological performance of the Mg matrix alloy. To date, several materials have been employed to reinforce the Mg-matrix composites including Al2O3, SiC, TiB2, and TiC, carbon nanotubes (CNTs), and graphite (which are commonly used as self-lubricants in the Mg-matrix composites). While single-reinforcement MMCs offer considerable improvements, recent research has focused on next-generation materials known as hybrid composites. Hybridization utilizes two or more distinct reinforcement phases—often a combination of a hard ceramic and a softer solid lubricant—to achieve synergistic property enhancement, offering a balanced combination of high strength and excellent wear characteristics.

Magnesium alloys, particularly the AZ series (AZ91D), are globally preferred in automotive and aerospace sectors for their exceptional high specific strength and lightweight nature. However, AZ91D suffers from poor wear resistance and relatively low hardness, restricting its use in high-performance structural applications.

In this context, the combination of Boron Carbide B_4C microparticles and Multi-Walled Carbon Nanotubes (MWCNTs) is highly promising. B_4C is renowned for its ultra-high hardness, high elastic modulus, and excellent thermal stability, making it an ideal primary load-bearing component that effectively resists abrasive wear and plastic deformation of the matrix. Conversely, MWCNTs, which possess superior tensile strength and ductility, are included to refine the grain structure and, most importantly, provide intrinsic self-lubricating properties. During dry sliding contact, MWCNTs are capable of exfoliating or shearing to form a thin, stable, protective tribo-layer (or mechanically mixed layer) on the worn surface. This mechanism effectively reduces the direct metal-to-metal contact, leading to a significant decrease in the coefficient of friction and specific wear rate. While the effects of these reinforcements individually on Mg alloys are well-documented, a comprehensive and systematic investigation into the synergistic effect of this specific micro- and nano-hybrid combination B_4C microparticles and MWCNTs on the overall tribological performance remains an area requiring in-depth study.

This study, therefore, aims to systematically investigate the synergistic effect of B_4C microparticles and MWCNTs on the microstructure, mechanical properties, and, most critically, the dry sliding tribological behaviour of the Mg-based hybrid composite. The research focuses on identifying the optimal composition and processing parameters necessary to maximize wear resistance and minimize the coefficient of friction. Furthermore, a detailed analysis of the worn surfaces, using techniques such as optical microscopy will be conducted to elucidate the dominant wear mechanisms (i.e., abrasion, adhesion, delamination, and the formation of the tribo-layer) under varying load and sliding speed conditions. The findings presented herein provide critical insights into the underlying wear mechanisms and optimal composition necessary for developing lightweight Mg composites with superior endurance for high-stress, dynamic applications.

The surge in demand for lightweight structural materials is fundamentally reshaping high-tech manufacturing, particularly in the mechanical and structural sectors (Sahu et al., 2020, Zhu et al., 2020 & Kianfar et al., 2020). For years, aluminium and its alloys have reigned supreme in critical applications like automotive, aerospace, and computer components, thanks to their exceptional strength-to-weight ratio. (Singh et al., 2020, Yuan et al., 2016, Aghaie et al., 2018, & Aghaie et al., 2019). However, a new contender is rising fast: magnesium (Mg) alloys. Offering the potential for even greater weight reduction than aluminium, Mg is proving irresistible to engineers. Beyond its light mass, it boasts superior properties like outstanding castability, high damping capacity, and easy machinability and recycling. Conversely, Mg may have relatively low mechanical properties, especially low tribological properties and poor fracture behaviours. (Tayebi et al., 2020, Tayebi et al., 2021, Pan et al., 2020, Mohammadi et al., 2015) Lately, the highest demand for Mg alloys and their composites is for certain automotive components such as pistons, brake system, and cylinder bores that requires high wear resistance (Jiang et al., 2012, Mohammadi et al., 2015, & Mohammadi et al., 2014). It is well known that sliding a soft material such as Mg against a hard material without lubrication may result in abrasion, or flow and adherence of the soft material to the hard one, creating an interface with low shear strength. These limitations lead to a short service time for Mg-based components and making Mg alloys unsuitable to be used for gears, pistons, bearings, and cylinder applications (Zhang et al., 2020, Nouri et al., 2017, & Sediako et al., 2019). The results of research on composites reinforced with hard ceramic particles have shown that with uniform distributions and strong interface, the addition of ceramic particles can reduce the wear rate. Proper wettability between the melt and reinforcement particles plays a significant role in the wear properties. Furthermore, the particle agglomeration in the melt during the solidification may lead to the formation of a nonuniform distribution. Nonuniformity of the reinforcement particles in the composite matrix also can be a result of chemical interaction between the ceramic particles and the solid/liquid interface movement (Maleki et al., 2015). Wettability is the foundational requirement for achieving robust bonding between the matrix and reinforcement particles during casting processes. Adequate wettability ensures a cohesive interface, promoting uniform reinforcement distribution and facilitating efficient load transfer from the matrix to the reinforcement phase, which is critical for preventing composite failure (Sabzi et al., 2018, Jafarian et al., 2021, Mousavi et al., 2018, Dezfuli et al., 2018).

Magnesium alloys, particularly the AZ series (AZ91D), are globally preferred in automotive and aerospace sectors for their exceptional high specific strength and lightweight nature. However, AZ91D suffers from poor wear resistance and relatively low hardness, restricting its use in high-performance structural applications. García-Rodríguez et al. investigated the dry sliding behaviour of AZ91 magnesium composites reinforced with 5 and 10 vol% SiCp across a wide range of conditions: Sliding Speeds: 0.1 to 1 m/s & Normal Loads: 10 to 250 N. The study identified abrasion, oxidation, delamination, and melt wear as the dominant mechanisms, which shifted depending on the applied load: Oxidation wear (Low load), Abrasion and delamination wears (Medium load) & Melt wear (high load). The AZ91 alloy, regardless of reinforcement, displayed similar wear mechanism transitions to samples with a dendritic microstructure. This suggests that the microstructure had an insignificant effect on the observed wear conditions. Under the most severe conditions (150–250 N load and 0.5–1 m/s speed), melt wear became dominant. This was a result of increased frictional heating leading to surface melting, a condition where the SiC particles did not reduce the wear rate. Increasing the SiC content to 10 vol% resulted in a notable difference: a delay in the transition to the delamination wear mechanism. This delay was attributed to the formation of an oxide layer with a different morphology on the AZ91/SiCp 10% composite surface. Labib et al. (Labib et al., 2016) evaluated the influence of SiC reinforcement on the wear behaviour of a pure Mg matrix fabricated via powder metallurgy, focusing on temperature and load: Temperature Range: 25ºC to 200ºC, Sliding Speed: 0.4 m/s, Normal Loads: 5 to 60 N. They reported a consistent transition

load of 20 N for all samples, marking the shift between two distinct wear regimes: Mild Wear Regime (Lower Loads): Dominated by oxidation wear. Severe Wear Regime (Above 20 N): Dominated by adhesion and severe plastic deformation.
A contemporary strategy in materials engineering focuses on developing self-lubricating MMCs to reduce frictional losses, primarily driven by the demands of the automotive sector. This involves incorporating particles of solid lubricants such as graphite, molybdenum disulfide, and carbon nanotubes (CNTs) as reinforcement phases to decrease the coefficient of friction (COF). The efficacy of these lubricants stems from their unique layered structure, which is characterized by weak interlayer Van der Waals bonding (Omrani et al., 2016, Rapoport et al., 1997). This structure facilitates low-strength shearing parallel to the sliding surface, providing minimum tangential resistance and consequently a low COF. However, a key limitation of relying solely on solid lubricants is their effect on wear resistance. Such soft reinforcements typically do not impart sufficient scratch resistance to the composite. Furthermore, their lubricating capability may be compromised or lost entirely when subjected to high contact loads or harsh operating environments. Achieving the requisite mechanical properties and exploiting the full potential of MMCs is critically dependent on the employed production technique, which dictates the quality of the reinforcement distribution. Techniques such as casting (Tayebi et al., 2021, Sharifi et al., 2017, Tayebi et al.,2020) and powder metallurgy (Tayebi M et al., 2019) are widely utilized. The stir casting method stands out as one of the most promising and commercially viable techniques for preparing MMCs. Its advantages include: Ability to produce parts with complex geometries, Low production cost, High production rate. A contemporary and highly effective strategy for optimizing the properties of metal matrix composites (MMCs) involves the utilization of hybrid reinforcement systems. This approach is designed to synergistically combine the beneficial characteristics of different reinforcement types, leading to a tailored set of optimal material properties, particularly improvements in strength and abrasion resistance.

The hybrid strategy typically involves the simultaneous incorporation of two distinct classes of particulates: Hard Ceramic Particles: These inclusions primarily function to increase the composite's inherent scratch resistance and bulk hardness .Solid Self-Lubricants: Materials like graphite or MoS_2 provide low shear strength layers that reduce the coefficient of friction (COF).The combined effect of these additions is the development of a material possessing superior scratch resistance which minimizes wear damage and reduced friction, resulting in a lower overall friction rate during operation. The presence of diverse reinforcement phases, often varying in dimension, size, and composition, within the soft metal matrix (e.g., aluminium or magnesium alloys) activates a range of strengthening mechanisms. The different particle characteristics enable the material to exploit multiple strengthening effects simultaneously, which may include: Grain Refinement: Particles restrict grain growth during solidification or processing. Dislocation Impediment: Hard particles serve as obstacles to dislocation movement. Load Transfer: Stiffer reinforcements carry a greater portion of the applied load. By combining these mechanisms, hybrid reinforcement effectively improves the material's overall strength beyond what a single reinforcement type could achieve.
Recent advancements in hybrid magnesium matrix composites (HMMCs) have demonstrated the efficacy of ceramic particulate reinforcement in enhancing structural integrity. Specifically, research on AZ91D/B4C/BN systems fabricated via squeeze casting reported that a hybrid combination of 9 wt.% B_4C and 3 wt.% BN resulted in a 77.43% improvement in corrosion resistance and a 40.8% increase in compressive strength compared to the monolithic alloy (Raj et al., 2025). While the BN/B4C system excels in corrosive environments due to the formation of protective oxide layers, the integration of MWCNTs offers a specialized advantage in tribological applications by forming a self-lubricating tribo-film that significantly lowers the coefficient of friction.

Aim of the current study was to assess the wear behaviour and the dominant wear mechanisms of the AZ91D magnesium matrix composites. The effect of variation of MWCNTs and B4C reinforcements on the tribological properties of AZ91D matrix composites was investigated. (a) Role of B_4C: Boron Carbide is utilized as a micro-reinforcement due to its near-diamond hardness, high elastic modulus, and thermal stability. It acts as the primary "load-bearer," significantly increasing hardness but often reducing ductility. (b) Role of MWCNTs: To overcome the brittleness introduced by micro-ceramics, MWCNTs are added. Their high aspect ratio and graphitic structure provide two benefits: nanoscale bridge strengthening and self-lubrication, which reduces the coefficient of friction (COF). Therefore, AZ91D hybrid composites were reinforced by B4C and various MWCNTs contents and the enhanced mechanical properties were evaluated to provide beneficial data regarding the development of lightweight Mg composites with high strength to minimize the COF and wear rate of MMCs. The attempts were made to attain valuable data to improve and develop industrial components for aerospace applications.

2. Materials and Methods

2.1. Composite Fabrication

A commercially available Mg alloy AZ91D was used as the matrix material. The chemical composition of the AZ91D alloy ingot is presented in Table 1. B_4C particles (average size: 50 µm) and MWCNTs (average diameter: 25 nm, length: 35 µm) were used as reinforcements. Hybrid composites with varying weight percentages (1.5 wt.% B_4C+ 0.2-0.4 wt.% MWCNT) were fabricated using the Bottom pouring stir casting technique. The samples designation is presented in Table 2. This method is preferred for achieving better dispersion and wettability of nano-reinforcements in the molten metal. To ensure effective incorporation and optimize the wetting behaviour between the ceramic reinforcements B_4C and MWCNT and the molten magnesium matrix, the cleaned and dispersed reinforcement mixture was subjected to a preheating treatment. The mixture was loaded into a preheating chamber and held at a temperature of 200°C for 30 minutes. This step was essential to remove any

adsorbed moisture or surface gases that could otherwise lead to undesirable reactions or porosity during the subsequent stir casting process. The AZ91D magnesium ingots were placed within a graphite crucible inside the stir casting furnace. The furnace chamber was sealed, and a highly controlled protective atmosphere was established to prevent the aggressive oxidation and combustion of the molten magnesium. The protective atmosphere was maintained using Argon. The alloy was heated until completely molten, reaching a superheat temperature in the range of 850°C. A mechanical stirrer was lowered into the molten metal. Stirring commenced at a moderate speed 500 rpm to generate a stable vortex on the surface of the melt. The preheated B_4C and MWCNT reinforcement mixture was gradually introduced into the vortex Following the introduction of the reinforcements, the stirring speed was increased to 600rpm and maintained for 10 minutes. This action was critical to promote the uniform wetting and homogeneous dispersion of the reinforcements throughout the molten AZ91D matrix, while simultaneously preventing particle agglomeration, sinking, or floating. The melt temperature was rigorously controlled and maintained within the superheat range throughout the entire mechanical stirring phase. After the specified stirring time, the mechanical agitation was ceased. The resulting homogeneous molten composite was immediately poured into a preheated steel mold.

Table 1. Chemical composition of AZ91D Alloy

Elements	Copper	Al	Si	Iron	Nickel	Zinc	Manganese	Mg
Wt. %	0.03	8.2	0.1	0.003	0.002	0.45	0.4	Bal.

Table 2. The designation of AZ91D matrix samples.

Designation	AZ91D	1.5/0.2	1.5/0.4
Reinforcement (wt. %)	B4C	1.5	1.5
	MWCNT	0.2	0.4

2.2. Density and Porosity Measurements

The physical properties of the hybrid AZ91D composites were evaluated to determine the impact of hybrid reinforcement on structural integrity. The skeletal (theoretical) density(ρ_t) and apparent (measured) density (ρ_a) were compared to calculate the percentage porosity (P). The theoretical density of the composites was calculated via dividing the sample mass by its volume and the average value was reported for each sample, while the experimental density was determined using Archimedes' principle. The porosity volume of the specimens was determined by Eq. (1) [39].

$$P = [1 - \rho_a / \rho_t] \times 100 \quad \ldots\ldots\ldots\ldots\ldots\ldots\ldots\ldots\ldots\ldots\ldots\ldots\ldots\ldots\ldots\ldots\ldots\ldots(1)$$

2.3. Microstructural Characterization

The microstructure of the as-cast composites was analysed using an optical Microscope. Microstructure analysis of the fabricated materials was done by utilizing an optical microscope. A specimen with a diameter of 10 mm and thickness of 5 mm was made by wirecut EDM machining. To obtain a smooth surface finish, the samples were prepared and polished using SiC sandpapers of different grades, and then an ultra-fine smooth surface finish was achieved by applying 1 µm diamond paste.

2.4. Hardness

Microhardness tests were conducted to assess the mechanical strength improvements due to the hybrid reinforcement. Microhardness of the specimens was measured using a Vickers microhardness tester under a 100-gm load and a dwell time of 15 s. For each composite type, three replicate measurements were performed and the average microhardness value was reported. A diamond indenter with a square-based pyramidal geometry (with a 136° angle between opposite faces) is pressed into the surface of the material using a specific load (often ranging from a few grams to 100g for micro hardness testing). The load is typically held for 15 sec. After removing the load, the two diagonals of the resulting impression are measured under a microscope. The mean diagonal length is used in calculations. The Vickers hardness (HV) is calculated using the formula:

$$\text{HV} = \frac{1.8544 \times F}{d2}$$

where, F is the applied force (in kgf), d is the average length of the diagonals (in mm)

2.5. Tribological Testing

Dry sliding wear tests were performed using a pin-on-disc tribometer according to the ASTM G99 standard. Composite specimens were prepared as pins, and a hardened steel disc (HRC 60) was used as the counter face. Samples were weighed using a high accuracy (0.0001g) digital electronic balance machine. The Coefficient of Friction (COF) was continuously monitored during the test.

REDVET - Revista electrónica de Veterinaria - ISSN 1695-7504
Vol 25, No. 2 (2024)
http://www.veterinaria.org
Article Received Revised- Accepted-

Figure 1. (a) AZ91D, (b) AZ91D/1.5 wt. % B_4C/0.2 wt. % MWCNT, (c) AZ91D/1.5 wt. % B_4C/0.4 wt. % MWCNT wear samples.

3. Results and Discussion

3.1 Density and Porosity

The physical properties of the hybrid AZ91D composites, specifically density and porosity, are critical indicators of the casting quality and the effectiveness of the bottom-pouring stir casting technique. The experimental results for the composites reinforced with 1.5 wt. % B_4C and varying concentrations of MWCNTs (0.2–0.4 wt. %) are listed in table 3.

Table 3. Demonstrates the variations of density and porosity for samples with different MWCNTs contents.

Material Composition	Theoretical Density (g/cm3)	Measured Density (g/cm3)	Relative Density (%)	Porosity (P%)
Pure AZ91D	1.810	1.782	98.45	1.55%
AZ91D + 1.5% B4C + 0.2% MWCNT	1.818	1.795	98.73	1.27%
AZ91D + 1.5% B4C + 0.4% MWCNT	1.821	1.802	98.95	1.05%

The measured density increased from 1.782 g/cm^3 to 1.802 g/cm^3. This upward trend is attributed to the presence of B_4C, which possesses a significantly higher density (approx 2.52 g/cm^3) than the magnesium matrix. While MWCNTs are lightweight, their exceptional dispersion at 0.4 wt. % contributes to the densification of the matrix. The relative density increases from 98.45% in the base alloy to 98.95% in the 0.4 wt. % MWCNT hybrid composite. This indicates a significant reduction in porosity. The improvement can be attributed to: (a) The bottom-pouring method and mechanical stirring at 600 rpm helped in purging gas bubbles and ensuring the molten metal effectively wetted the reinforcements. (b) Preheating the B_4C/MWCNT mixture to 200ºC successfully removed surface moisture, preventing the formation of hydrogen pores during solidification. The porosity of the specimens decreased from 1.55% to 1.05%. This 32.2% reduction in porosity compared to the unreinforced alloy highlights the effectiveness of the processing parameters. The nanoscale MWCNTs likely act as a filler for micro-voids formed at the interfaces of the larger B_4C particles, leading to higher apparent density measurements.

3.2. Microstructural Characterization

The optical microscopy analysis was employed to examine the distribution of reinforcements and the grain morphology of the monolithic AZ91D alloy and its hybrid composites (reinforced with 1.5 wt. % B_4C and 0.2–0.4 wt. % MWCNT). Microstructural analysis in Fig 2. revealed uniform distribution of both B_4C microparticles and MWCNTs within the Mg matrix, though some minimal agglomeration of MWCNTs was observed. The presence of hard B_4C particles acts as a barrier to the movement of dislocations and effectively refines the grain structure of the Mg matrix. Table 4 interprets the microstructural features of samples.

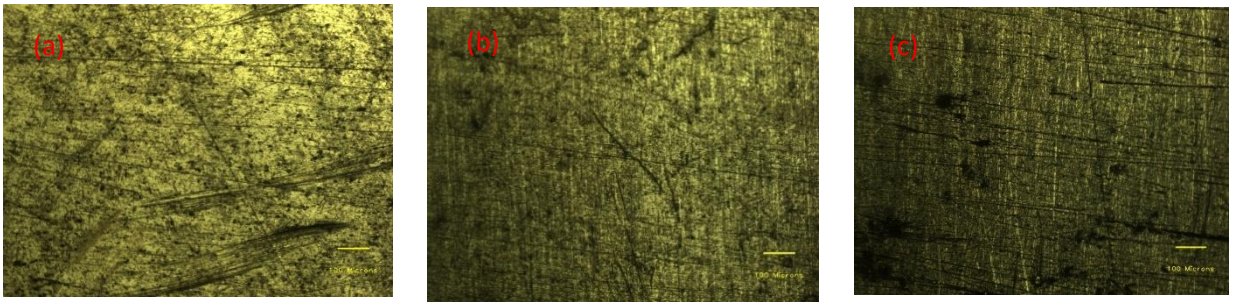

Figure 2. Optical micrographs of: (a) AZ91D, (b) AZ91D/1.5 wt. % B_4C/0.2 wt. % MWCNT, (c) AZ91D/1.5 wt. % B_4C/0.4 wt. % MWCNT samples.

REDVET - Revista electrónica de Veterinaria - ISSN 1695-7504
Vol 25, No. 2 (2024)
http://www.veterinaria.org
Article Received Revised- Accepted-

Table 4. Optical microscopy summary

Sample ID	Major Microstructural Features	Grain Size Assessment
Pure AZ91D	Coarse dendrites, continuous β network	Coarse
AZ91D + 1.5% B4C+ 0.2% MWCNT	Refined dendrites, uniform B4C distribution	Medium-Fine
AZ91D + 1.5% B4C + 0.4% MWCNT	Highly refined grains, discrete β precipitates	Ultra-Fine

3.2.1. Matrix Grain Refinement

The unreinforced AZ91D alloy exhibited a characteristic coarse dendritic structure consisting of the primary α -Mg phase and a eutectic β ($Mg_{17}Al_{12}$) phase distributed along the grain boundaries. Upon the addition of 1.5 wt. % B_4C, significant grain refinement was observed. This refinement progressed with the incorporation of MWCNTs, where the sample containing 0.4 wt. % MWCNT showed the finest grain structure. This effect is attributed to two primary mechanisms. (a). Heterogeneous Nucleation: The B_4C microparticles and MWCNTs act as potent nucleation sites during the solidification of the molten magnesium, increasing the number of nuclei and restricting the growth of grains. (b). Restricted Growth: The physical presence of MWCNTs at the grain boundaries impedes the migration of boundaries, resulting in a more refined and equiaxed microstructure.

3.2.2. Reinforcement Distribution

The hybrid composites displayed a generally uniform dispersion of B_4C particles throughout the magnesium matrix. At 0.2 wt. % MWCNT, the nanotubes were observed predominantly in the inter-dendritic regions. Increasing the MWCNT content to 0.4 wt. % maintained a homogeneous distribution, although localized clusters were noted at higher magnifications, common in nano-reinforced composites.

3.2.3. Interfacial Integrity

Optical micrographs confirmed robust interfacial bonding, characterized by the absence of visible voids or micro-cracks at the particle-matrix interfaces. The formation of the β-phase was also observed to be modified; instead of the continuous network found in the base alloy, it appeared as finer, more discrete precipitates in the hybrid composites, potentially indicating a beneficial interaction between the reinforcement surface and the alloying elements.

3.3. Microhardness

The measured microhardness (Table-5) showed a substantial improvement in the hybrid composites compared to the monolithic Mg alloy AZ91D. The microhardness measurements for the AZ91D composites reinforced with 1.5 wt.% B_4C and varying amounts of multi-walled carbon nanotubes (MWCNTs) are presented in fig. 3. A notable and consistent increase in microhardness was observed with the addition of both B_4C and MWCNTs compared to the monolithic AZ91D alloy (Fig. 4). The maximum microhardness was achieved in the hybrid composite containing 1.5 wt. B_4C and 0.4 wt. % MWCNT. Specifically, the microhardness of this optimal composition reached a value of 115.9 HV compared to the base AZ91D alloy 82.7 HV A clear trend of increasing microhardness was observed as the MWCNT content was raised from 0.2 wt.% to 0.4 wt. %. The significant increase in microhardness of the AZ91D-B_4C-MWCNT hybrid composites, particularly at the 0.4 wt. % MWCNT addition, can be primarily attributed to the combined effects of the hard ceramic reinforcements and the synergistic strengthening mechanisms they induce.

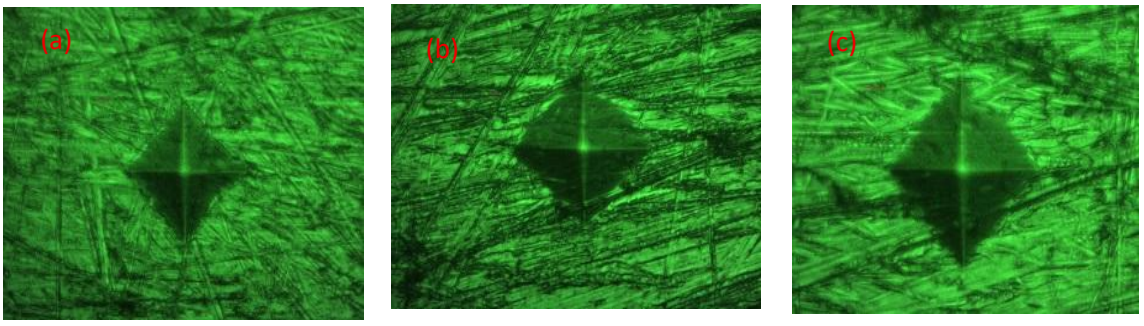

Figure 3. Shows indentations on the specimens; (a). AZ91D; (b). AZ91D/1.5 wt. % B_4C/0.2 wt. % MWCNT; (c). AZ91D/1.5 wt. % B_4C/0.4 wt. % MWCNT

Table 5. Measurement of microhardness

Sample	d1 (µm)	d2 (µm)	Mean dia. (µm)	Hardness (HV)
AZ91D	54.88	39.79	47.335	82.71
AZ91D/1.5 wt. % B_4C/0.4wt. % MWCNT	48.93	43.45	46.19	86.97
AZ91D/1.5 wt. % B_4C/0.2 wt. % MWCNT	41.92	38.11	40.015	115.9

REDVET - Revista electrónica de Veterinaria - ISSN 1695-7504
Vol 25, No. 2 (2024)
http://www.veterinaria.org
Article Received Revised- Accepted-

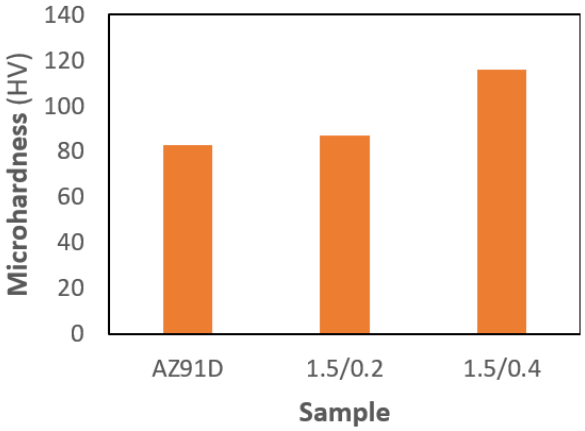

Figure 4. Microhardness of AZ91D unreinforced and B_4C-MWCNT/AZ91D composites samples.

3.3.1 Effect of Hard B_4C Particles

The incorporation of 1.5 wt. % B_4C acts as the primary stiffening agent. B_4C possesses exceptionally high hardness and elastic modulus. Its presence within the softer AZ91D magnesium matrix resists the plastic deformation induced by the Vickers indenter, which is the direct cause of the hardness increase. This is primarily described by the load-bearing effect, where the hard ceramic particles carry a significant portion of the applied load.

3.3.2 Role of MWCNTs (Nanoscale Strengthening)

The subsequent increase in microhardness upon the addition of MWCNTs is due to their nanoscale geometry and superior mechanical properties. Carbon nanotubes have an extremely high aspect ratio and mechanical strength, making them highly effective reinforcements, even at very low weight percentages. The peak microhardness at 0.4 wt. % MWCNT suggests this concentration represents an optimal balance between reinforcement effect and dispersion quality. At this level, the MWCNTs are likely well-dispersed within the matrix and at the grain boundaries, maximizing their strengthening contribution. The reinforcement particles, particularly the fine MWCNTs, can act as heterogeneous nucleation sites during solidification, leading to a finer grain structure in the AZ91D matrix. According to the Hall-Petch effect, a reduced grain size increases the yield strength and hardness. The non-deformable B_4C particles and MWCNTs act as formidable obstacles to dislocation motion in the magnesium matrix. Dislocations are forced to bypass these nanoparticles, leading to an increase in flow stress and, consequently, microhardness. The magnitude of this effect is inversely related to the particle spacing, which is reduced by the addition of MWCNTs. The significant difference in the Coefficient of Thermal Expansion (CTE) between the AZ91D matrix and the reinforcements B_4C and MWCNT) generates a high density of geometrically necessary dislocations (GNDs) near the particle-matrix interface upon cooling from the processing temperature. [20-22]. This increased dislocation density contributes to work hardening and a higher measured hardness.

3.3.3. Synergistic Hybrid Effect

The hybrid reinforcement B_4C and MWCNT appears to offer a synergistic effect, outperforming the effect of B_4C alone. The MWCNTs, in addition to contributing directly to strengthening, likely improve the overall interface quality and load transfer between the B_4C particles and the matrix, leading to the superior microhardness observed. The nanoscale MWCNTs may occupy interstitial positions between the larger B_4C particles, promoting a more uniform stress distribution.

3.4. Coefficient of Friction (COF)

The tribological performance of the AZ91D magnesium alloy and its hybrid composites was evaluated to determine the influence of B_4C and MWCNT reinforcements on the Coefficient of Friction (COF). The experimental data reveals a significant improvement in the frictional characteristics of the AZ91D alloy upon the addition of reinforcements. The measured COF values are summarized in the table 6.

Table 6. Average COF of B4C-MWCNT/AZ91D composites with various contents

Material Composition	Weight % of MWCNT	Avg. Coefficient of Friction (COF)	% Reduction vs. Base Alloy
Pure AZ91D (Unreinforced)	0%	0.312	-
AZ91D + 1.5% B4C+ 0.2% MWCNT	0.2%	0.278	~10.9%
AZ91D + 1.5% B4C+ 0.4% MWCNT	0.4%	0.261	~16.3%

The base AZ91D alloy exhibits the highest COF (0.312), attributed to the relatively soft magnesium matrix which undergoes significant plastic deformation and metal-to-metal contact during sliding. The introduction of 1.5 wt % B_4C serves as a hard secondary phase. These particles act as load-bearing elements, reducing the real area of contact between the pin and the

counterface, thereby initiating a decrease in friction. The most notable observation is the further reduction in COF as the MWCNT content increases from 0.2% to 0.4%. MWCNTs possess a unique hexagonal graphitic structure that allows for easy shearing between layers. During the sliding process, MWCNTs are squeezed out from the matrix to form a thin, stable solid lubricant film (tribo-layer) on the sliding surface. Some MWCNTs may act as "nanoscale ball bearings" between the contact surfaces, converting sliding friction into rolling friction, which significantly lowers the COF to its minimum value of 0.261 in the 0.4 wt. % MWCNT sample. The decrease from 0.278 to 0.261 as MWCNT content doubles suggests that 0.4 wt.% provides a more continuous and uniform lubricant film. At 0.2%, the film may be intermittent, allowing more direct contact between the hard B_4C particles or the matrix and the counterface. The hybrid reinforcement strategy successfully combines the hardness of B_4C with the self-lubricating properties of MWCNTs to optimize the wear resistance of the AZ91D alloy. The variation of coefficient of friction (COF) with respect to time is shown in Figure 5.

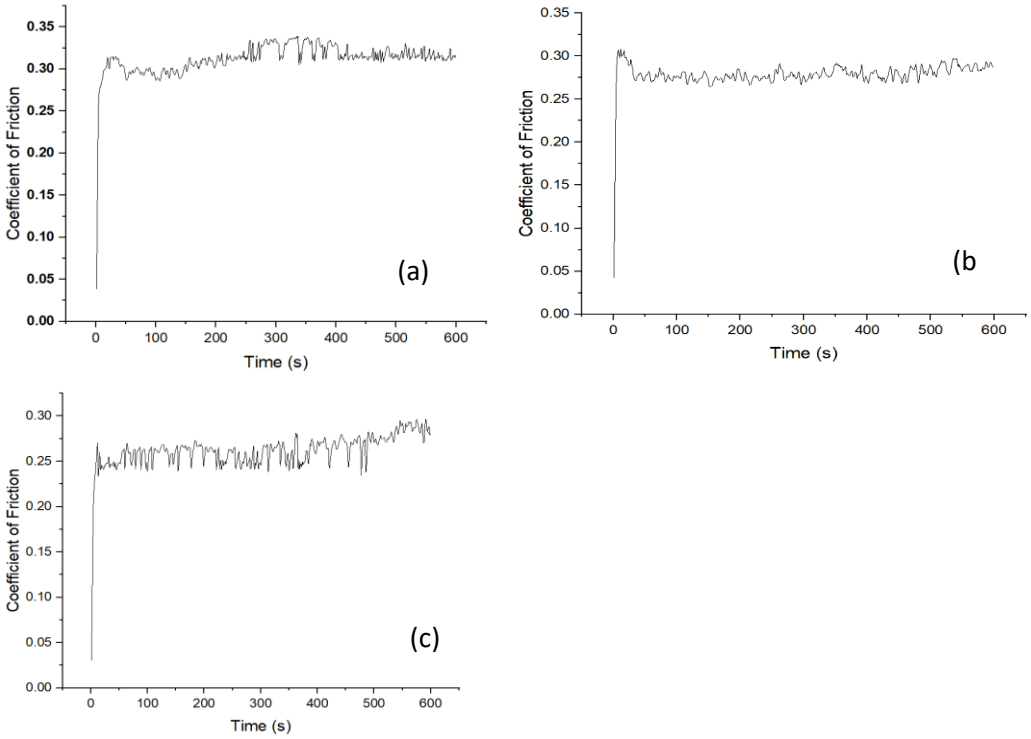

Figure 5. Variation in COF with respect to time for AZ91D unreinforced and B_4C-MWCNT/AZ91D composites samples.

3.4 Wear

A notable reduction in the wear was observed as the MWCNT concentration increased as shown in Fig. 6. The wear loss is the mass loss (gram) of the specimen after conducting wear tests. Initial and final weight of sample is shown in Table 7.

Table 7. Calculation of wear

Sample	Initial weight (gram)	Final weight (gram)	Wear (gram)
AZ91D	6.4015	6.3968	0.0047
1.5/0.2	6.9001	6.8967	0.0034
1.5/0.4	6.8039	6.8011	0.0028

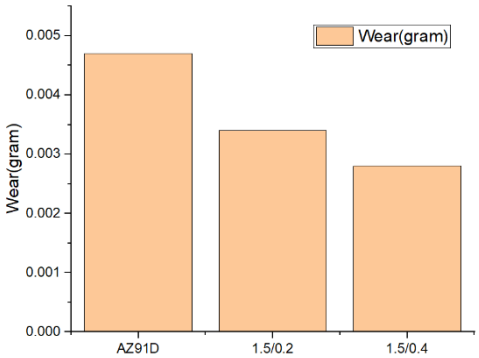

Figure 6. Variation of wear for AZ91D unreinforced and B_4C-MWCNT/AZ91D composites samples.

4. Conclusion

The fabrication of hybrid magnesium matrix composites (AZ91D reinforced with 1.5 wt. % B_4C and varying concentrations of MWCNTs) using a controlled bottom-pouring stir casting technique successfully yielded materials with significantly enhanced tribological properties.

The following key findings were established:

1. Fabrication and Densification: Hybrid AZ91D composites reinforced with 1.5 wt.% B_4C and 0.2–0.4 wt. % MWCNTs were successfully fabricated via bottom-pouring stir casting. The preheating treatment and protective Argon atmosphere resulted in a high degree of structural integrity, with porosity levels decreasing from 1.55% in the base alloy to 1.05% in the optimized hybrid composite.

2. Microstructural Refinement: The fabrication process, assisted by protective Argon atmosphere and preheating of reinforcements, resulted in a generally uniform distribution of B_4C microparticles and MWCNTs within the AZ91D matrix. The inclusion of ceramic microparticles and carbon nanotubes served as effective heterogeneous nucleation sites, resulting in significant grain refinement of the α-Mg matrix. The MWCNTs, in particular, restricted grain growth at the boundaries, creating a more equiaxed and refined dendritic structure.
3. Mechanical Enhancement: The introduction of reinforcements led to a significant increase in microhardness. The composite containing 1.5 wt.% B_4C and 0.4 wt. % MWCNT achieved the peak hardness of 115.9 HV, representing a 40.1% increase over the monolithic AZ91D alloy (82.7 HV). This improvement is attributed to the synergistic effects of load-bearing B_4C particles, Hall-Petch grain refinement, and the high dislocation density generated by the mismatch in thermal expansion coefficients.
4. Tribological Optimization: A notable reduction in the Coefficient of Friction (COF) was observed as the MWCNT concentration increased. The base alloy COF of 0.312 was reduced to 0.261 for the 0.4 wt. % MWCNT hybrid composite, marking a 16.3% improvement. Multi-Walled Carbon Nanotubes (MWCNTs) act as an effective solid lubricant, forming a stable carbon-rich tribo-layer on the sliding surface, which is critical for reducing the coefficient of friction and minimizing adhesive wear.
5. Self-Lubrication Mechanism: The friction reduction is driven by the formation of a stable, graphitic tribo-layer on the sliding surface and the potential "ball-bearing" effect of nanotubes, which effectively prevents direct metal-to-metal contact.

Summary

The hybrid reinforcement strategy utilizing B_4C for structural stiffness and MWCNTs for both strength and lubrication provides a highly effective route for enhancing the mechanical and tribological performance of AZ91D alloys for high-performance applications. The hybridization of AZ91D with B_4C and MWCNTs provides a tailored solution for lightweight structural applications. The structural stiffness provided by B_4C and the lubrication/scale-reinforcement provided by MWCNTs create a synergistic effect that no single reinforcement can match. Future research should focus on multi-directional forging or extrusion to further refine the microstructure of these hybrid composites.

References

1. Aghaie, E. (2019). *Effect of cerium addition on improvement of mechanical properties of B319 powertrain aluminum alloy*. (Doctoral dissertation, University of Toronto).
2. Aghaie, E., Stroh, J., Sediako, D., & Smith, M. (2018). In-situ fitness-for-service assessment of aluminum alloys developed for automotive powertrain lightweighting. In O. Martin (Ed.), *Light metals 2018* (pp. 397–400). Springer International Publishing. https://doi.org/10.1007/978-3-319-72481-5_57
3. Archard, J. F. (1953). Contact and rubbing of flat surfaces. *Journal of Applied Physics*, *24*(8), 981–988. https://doi.org/10.1063/1.1721448
4. Bayati, M. S., Sharifi, H., Tayebi, M., & Isfahani, T. (2019). Effect of Al-B4C nanocomposite filler manufactured by accumulative roll bonding (ARB) method on the microstructure and mechanical properties of weldings prepared by tungsten inert gas welding. *Materials Research Express*, *6*(10), 106529. https://doi.org/10.1088/2053-1591/ab3dfa
5. Dezfuli, S. M., & Sabzi, M. (2018). Effect of yttria and benzotriazole doping on wear/corrosion responses of alumina-based nanostructured films. *Ceramics International*, *44*(16), 20245–20258. https://doi.org/10.1016/j.ceramint.2018.07.241
6. García-Rodríguez, S., Torres, B., Maroto, A., L´opez, A. J., Otero, E., & Rams, J. (2017). Dry sliding wear behavior of Globular AZ91 magnesium alloy and AZ91/SiCp composites. *Wear*, *390–391*, 1–10. https://doi.org/10.1016/j.wear.2017.08.017
7. Guo, Y., Wang, S., Liu, W., Sun, Z., Zhu, G., & Xiao, T. (2020). Effect of laser shock peening on tribological properties of magnesium alloy ZK60. *Tribology International*, *144*, 106138. https://doi.org/10.1016/j.triboint.2019.106138
8. Jafarian, H. R., Sabzi, M., Mousavi Anijdan, S. H., Eivani, A. R., & Park, N. (2021). The influence of austenitization temperature on microstructural developments, mechanical properties, fracture mode and wear mechanism of hadfield

high manganese steel. *Journal of Materials Research and Technology*, *10*, 819–831. https://doi.org/10.1016/j.jmrt.2020.11.086
9. Jiang, J., Wang, Y., Li, Y., Shan, W., & Luo, S. (2012). Microstructure and mechanical properties of the motorcycle cylinder body of AM60B magnesium alloy formed by combining die casting and forging. *Materials & Design*, *37*, 202–210. https://doi.org/10.1016/j.matdes.2012.01.002
10. Khakzad, A., Mousavi Khoi, S. M., Tayebifard, S. A., Aghaie, E., Behnamian, Y., Mozammel, M., & Ashrafizadeh, S. A. (2017). Alumina-silica composite coatings on aluminum by plasma electrolytic oxidation: the effect of coating time on microstructure, phase, and corrosion behavior. *Journal of Materials Engineering and Performance*, *26*(6), 2663–2670. https://doi.org/10.1007/s11665-017-2646-6
11. Kianfar, S., Aghaie, E., Stroh, J., Sediako, D., & Tjong, J. (2021). Residual stress, microstructure, and mechanical properties analysis of HPDC aluminum engine block with cast-in iron liners. *Materials Today Communications*, *26*, 101814. https://doi.org/10.1016/j.mtcomm.2020.101814
12. Labib, F., Ghasemi, H. M., & Mahmudi, R. (2016). Dry tribological behavior of Mg/SiCp composites at room and elevated temperatures. *Wear*, *348–349*, 69–79. https://doi.org/10.1016/j.wear.2015.11.004
13. Luo, H., Leitch, M., Behnamian, Y., Ma, Y., Zeng, H., & Luo, J-L. (2015). Development of electroless Ni–P/Nano-WC composite coatings and investigation on its properties. *Surface and Coatings Technology*, *277*, 99–106. https://doi.org/10.1016/j.surfcoat.2015.07.042
14. Maleki-Ghaleh, H., Hafezi, M., Hadipour, M., Nadernezhad, A., Aghaie, E., Behnamian, Y., & Mohanna, S. (2015). Effect of tricalcium magnesium silicate coating on the electrochemical and biological behavior of Ti-6Al-4V alloys. *PLoS ONE*, *10*(9), e0138454. https://doi.org/10.1371/journal.pone.0138454
15. Mohammadi, J., Behnamian, Y., Mostafaei, A., & Gerlich, A. P. (2015). Tool geometry, rotation and travel speeds effects on the properties of dissimilar magnesium/aluminum friction stir welded lap joints. *Materials & Design*, *75*, 95–112. https://doi.org/10.1016/j.matdes.2015.03.003
16. Mohammadi, J., Behnamian, Y., Mostafaei, A., Izadi, H., Saeid, T., Kokabi, A. H., & Emamy, M. (2015). Friction stir welding joint of dissimilar materials between AZ31B magnesium and 6061 aluminum alloys: microstructure studies and mechanical characterizations. *Materials Characterization*, *101*, 189–207. https://doi.org/10.1016/j.matchar.2015.01.037
17. Mohammadi, J., Ghoreishi, M., & Behnamian, Y. (2014). An investigation into the dissolution characteristics of gamma precipitates in Mg-3Al-Zn alloy. *Materials Research*, *17*, 996–1002. https://doi.org/10.1590/1516-1439.277813
18. Mousavi Anijdan, S. H., & Sabzi, M. (2018). The effect of pouring temperature and surface angle of vortex casting on microstructural changes and mechanical properties of 7050Al- 3 wt% SiC composite. *Materials Science and Engineering: A*, *737*, 230–235. https://doi.org/10.1016/j.msea.2018.09.006
19. Nouri, M., & Li, D. Y. (2017). Maximizing the benefit of aluminizing to AZ31 alloy by surface nanocrystallization for elevated resistance to wear and corrosive wear. *Tribology International*, *111*, 211–219. https://doi.org/10.1016/j.triboint.2017.06.014
20. Omrani, E., Moghadam, A. D., Menezes, P. L., & Rohatgi, P. K. (2016). Influences of graphite reinforcement on the tribological properties of self-lubricating aluminum matrix composites for green tribology, sustainability, and energy efficiency—a review. *International Journal of Advanced Manufacturing Technology*, *83*(1), 325–346. https://doi.org/10.1007/s00170-015-7632-1
21. Pan, C., Wang, X., Behnamian, Y., Wu, Z., Qin, Z., Xia, D-H., & He, J. (2020). Monododecyl phosphate film on LY12 aluminum alloy: PH-controlled self-assembly and corrosion resistance. *Journal of the Electrochemical Society*, *167*(16), 161510. https://doi.org/10.1149/1945-7111/abb3f6
22. Raj, P. P., Ramadoss, N., Shoba, M. K., & Prabu, A. D. (2025). Enhancement of Mechanical and Corrosion Behaviours of AZ91D Magnesium Hybrid Composites Reinforced with B4C and BN Particles. *Inter Metalcast*, *19*, 3607–3620. https://doi.org/10.1007/s40962-025-01514-4
23. Rapoport, L., Bilik, Y., Feldman, Y., Homyonfer, M., Cohen, S. R., & Tenne, R. (1997). Hollow nanoparticles of WS2 as potential solid-state lubricants. *Nature*, *387*(6635), 791–793. https://doi.org/10.1038/387791a0
24. Sabzi, M., Dezfuli, S. M., & Far, S. M. (2018). Deposition of Ni-tungsten carbide nanocomposite coating by TIG welding: characterization and control of microstructure and wear/ corrosion responses. *Ceramics International*, *44*(18), 22816–22829. https://doi.org/10.1016/j.ceramint.2018.09.076
25. Sahu, P. K., Singh, S., Chen, G., Yijun, L., Zhang, S., & Shi, Q. (2020). Wear behavior of the friction stir alloyed AZ31 Mg at different volume fractions of Al particles reinforcement and its enhanced quality attributes. *Tribology International*, *146*, 106268. https://doi.org/10.1016/j.triboint.2020.106268
26. Sediako, D., Stroh, J., McDougall, A., & Aghaie, E. (2019). Residual stress analysis of A362 aluminum alloy gear case using neutron diffraction. *Materials Science Forum*, *941*, 1288–1294. https://doi.org/10.4028/www.scientific.net/MSF.941.1288
27. Sharifi, H., Ostovan, K., Tayebi, M., & Rajaee, A. (2017). Dry sliding wear behavior of open-cell Al-Mg/Al2O3 and Al-Mg/SiC-Al2O3 composite preforms produced by a pressureless infiltration technique. *Tribology International*, *116*, 244–255. https://doi.org/10.1016/j.triboint.2017.07.032

28. Shen, M. J., Wang, X. J., Zhang, M. F., Zhang, B. H., Zheng, M. Y., & Wu, K. (2015). Microstructure and room temperature tensile properties of 1 μm-SiCp/AZ31B magnesium matrix composite. *Journal of Magnesium and Alloys*, *3*(2), 155–161. https://doi.org/10.1016/j.jma.2015.06.004
29. Singh, H., & Bhowmick, H. (2020). Lubrication characteristics and wear mechanism mapping for hybrid aluminium metal matrix composite sliding under surfactant functionalized MWCNT-Oil. *Tribology International*, *145*, 106152. https://doi.org/10.1016/j.triboint.2019.106152
30. Tayebi, M., Bizari, D., & Hassanzade, Z. (2020). Investigation of mechanical properties and biocorrosion behavior of in situ and ex situ Mg composite for orthopedic implants. *Materials Science and Engineering: C*, *113*, 110974. https://doi.org/10.1016/j.msec.2020.110974
31. Tayebi, M., Jozdani, M., & Mirhadi, M. (2019). Thermal expansion behavior of Al–B4C composites by powder metallurgy. *Journal of Alloys and Compounds*, *809*, 151753. https://doi.org/10.1016/j.jallcom.2019.151753
32. Tayebi, M., Najafi, H., Nategh, S., & Khodabandeh, A. (2021). Creep behavior of ZK60 alloy and ZK60/SiCw composite after extrusion and precipitation hardening. *Metals and Materials International*, *27*(12), 3905–3917. https://doi.org/10.1007/s12540-020-00877-5
33. Tayebi, M., Nategh, S., Najafi, H., & Khodabandeh, A. (2020). Tensile properties and microstructure of ZK60/SiCw composite after extrusion and aging. *Journal of Alloys and Compounds*, *830*, 154709. https://doi.org/10.1016/j.jallcom.2020.154709
34. Tayebi, M., Tayebi, M., Rajaee, M., Ghafarnia, V., & Rizi, A. M. (2021). Improvement of thermal properties of Al/Cu/SiC composites by tailoring the reinforcement microstructure and comparison to thermoelastic models. *Journal of Alloys and Compounds*, *853*, 156794. https://doi.org/10.1016/j.jallcom.2020.156794
35. Wang, X. J., Wang, N. Z., Wang, L. Y., Hu, X. S., Wu, K., Wang, Y. Q., & Sun, Y. T. (2014). Processing, microstructure and mechanical properties of Micro-SiC particles reinforced magnesium matrix composites fabricated by stir casting assisted by ultrasonic treatment processing. *Materials & Design*, *57*, 638–645. https://doi.org/10.1016/j.matdes.2014.01.076
36. Yuan, L., Han, J., Liu, J., & Jiang, Z. (2016). Mechanical properties and tribological behavior of aluminum matrix composites reinforced with In-Situ AlB2 particles. *Tribology International*, *98*, 41–47. https://doi.org/10.1016/j.triboint.2016.02.012
37. Zare, R., Sharifi, H., Saeri, M. R., & Tayebi, M. (2019). Investigating the effect of SiC particles on the physical and thermal properties of Al6061/SiCp composite. *Journal of Alloys and Compounds*, *801*, 520–528. https://doi.org/10.1016/j.jallcom.2019.05.334
38. Zhang, Y., Chen, F., Zhang, Y., & Du, C. (2020). Influence of graphene oxide additive on the tribological and electrochemical corrosion properties of a PEO coating prepared on AZ31 magnesium alloy. *Tribology International*, *146*, 106135. https://doi.org/10.1016/j.triboint.2019.106135
39. Zhu, J., Qi, J., Guan, D., Ma, L., & Dwyer-Joyce, R. (2020). Tribological behaviour of self-lubricating mg matrix composites reinforced with silicon carbide and tungsten disulfide. *Tribology International*, *146*, 106253. https://doi.org/10.1016/j.triboint.2020.106253